remote sensing

MDPI

Article

Developing an Ensemble Precipitation Algorithm from Satellite Products and Its Topographical and Seasonal Evaluations Over Pakistan

Khalil Ur Rahman, Songhao Shang *, Muhammad Shahid and Jiang Li

State Key Laboratory of Hydroscience and Engineering, Department of Hydraulic Engineering, Tsinghua University, Beijing 100084, China; hlrhm17@mails.tsinghua.edu.cn (K.U.R.); shahidbaloch21@gmail.com (M.S.); lj397947820@163.com (J.L.)

* Correspondence: shangsh@tsinghua.edu.cn; Tel.: +86-10-6279-6674

Received: 15 October 2018; Accepted: 14 November 2018; Published: 20 November 2018

check for updates

Abstract: Accurate estimation of precipitation is critical for hydrological, meteorological, and climate models. This study evaluates the performance of satellite-based precipitation products (SPPs) including Global Precipitation Measurement (GPM)-based Integrated Multi-Satellite Retrievals for GPM (IMERG), Tropical Rainfall Measurement Mission (TRMM) Multi-Satellite Precipitation Analysis (TMPA 3B43-v7), Precipitation Estimation from Remotely-Sensed Information using Artificial Neural Network (PERSIANN), and PERSIANN-CDR (Climate Data Record), over Pakistan based on Surface Precipitation Gauges (SPGs) at spatial and temporal scales. A novel ensemble precipitation (EP) algorithm is developed by selecting the two best SPPs using the Paired Sample *t*-test and Principal Component Analysis (PCA). The SPPs and EP algorithm are evaluated over five climate zones (ranging from glacial Zone-A to hyper-arid Zone-E) based on six statistical metrics. The result indicated that IMERG outperformed all other SPPs, but still has considerable overestimation in the highly elevated zones (+20.93 mm/month in Zone-A) and relatively small underestimation in the arid zone (−2.85 mm/month in Zone-E). Based on the seasonal evaluation, IMERG and TMPA overestimated precipitation during pre-monsoon and monsoon seasons while underestimating precipitation during the post-monsoon and winter seasons. However, the developed EP algorithm significantly reduced the errors both on spatial and temporal scales. The only limitation of the EP algorithm is relatively poor performance at high elevation as compared to low elevations.

Keywords: satellite precipitation; Global Precipitation Measurement (GPM); IMERG; TRMM-TMPA; Ensemble Precipitation (EP) algorithm; topographical and seasonal evaluation

1. Introduction

Precipitation is crucial input parameter of the global hydrological cycle [1,2] and an impetuous factor contributing to natural disasters like droughts and flooding [3]. The performance of different hydrological, meteorological, and climate models depends on the accuracy of precipitation inputs. These models are used in reliable modeling, monitoring, and quantification of floods, drought assessment, landslides, agricultural production, and sustainable water resource management. Moreover, understanding of the spatial and temporal variability of precipitation is significantly important under climate change [4,5]. The spatial and temporal variation in precipitation pattern significantly affects socioeconomic factors such as disaster management, food security, ecosystem health, and hydropower generation [6–8]. Therefore, accurate precipitation estimation with high spatiotemporal resolution on a regional scale is essential for significant hydrological predictions. However, this is still a challenging task for the developing countries like Pakistan because of the sparse surface precipitation gauge (SPG) network and highly complex topography [9–11].

Most widely used techniques for precipitation measurement are in situ measurements (SPGs), and commercial microwave products such as ground-based radars and satellite-based sensors [4,12]. There are numerous errors associated with distribution and readings of SPG as discussed in [13]. Furthermore, the SPG measurements are in situ, which is difficult to describe the spatial variations in precipitation on a regional scale. To overcome these uncertainties, the utilization of satellite-based precipitation products (SPPs) to measure global or regional precipitation has increased significantly over the past thirty years [14]. In poorly or ungauged regions, SPP estimation techniques may be opted due to unavailability, uncertainty, and quantitative self-consistency of SPG data [15]. At present, the development of high-resolution SPPs has provided unprecedented opportunity to monitor the spatiotemporal variability in precipitation on a global scale, particularly at high elevation where ground-based information is scarce or not readily available [16–18]. A detailed description of the most widely used SPPs can be found in a past work [19].

A number of researchers evaluated the performance of these SPPs on the regional and global scales, such as Asia [3,20–23], Africa [24–26], North and South America [27–30], Europe [31–34], Australia [35–37], and others [14,38–41]. These studies conclude that GPM IMERG showed better performances than TRMM products across many countries of the world with different climatic conditions. Most of the SPPs showed weak performance in precipitation detection and resulted in high mean errors in regions having rapid precipitation gradients with complex terrain.

A very few studies are conducted over Pakistan [9–11,42–44]. Cheema and Bastiaanssen [9] calibrated TRMM-TMPA on a monthly time scale over the Indus Basin for runoff and soil water balance studies. Results revealed that TMPA overestimated the precipitation in high ranges and foothill plains, whereas underestimated precipitation in northwest and coastal areas compared with SPG data. Khan et al. [11] conducted a study to assess TMPA-v7 Real Time (RT) and Adjusted (Adj) TMPA and CMORPH-RT during the monsoon season on a daily temporal scale. The result revealed that TMPA-Adj v7 and CMORPH overestimated the precipitation over high altitudes in the study area. Overall, TMPA-v7 performed well as compared to other precipitation products. Anjum et al. [44] assessed the improvements of TMPA-v7 over TMPA-v6 on a basin scale study over the Swat River watershed (14,039 km^2). Results showed that both the magnitude and spatial variation were not captured accurately using TMPA-v7 and v6 on the annual and seasonal scales. However, both the products showed improved accuracy on a monthly time scale than daily precipitation estimate. Hussain et al. [43] evaluated the performance of CMORPH, TMPA, and PERSIANN data sets over three geomorphological climate zones: plain, mountain and glacial regions of Pakistan. Their results indicated that all SPPs captured the precipitation pattern accurately but overestimated the precipitation at glacial, whereas good performance over the mountain region as compared to plain zones. Furthermore, they concluded that the Adjusted (Adj) versions of SPPs outperformed their respective real-time (RT) versions. Muhammad et al. [42] proposed an ensemble algorithm based quantification of precipitation and assigned relative regional performance weights to IMERG research (IR), IMERG real-time (IT), and TRMM 3B42 (RT) to produce regional precipitation (RP) estimates. The results showed that the proposed RP algorithm provided significant agreement with SPG observations. Iqbal and Athar [10] validated TRMM-TMPA with SPG data and Asian Precipitation-Highly-Resolved Observational Data Integration Towards Evaluation of Water Resources (APHRODITE) named as APH data. The result revealed that TMPA slightly overestimated the precipitation at daily, monthly and annual scales compared with SPG and APH based observations, but the correlation with SPG observation was stronger compared with APH. Based on the seasonal evaluation, TMPA overestimated both SPG and APH based observations during the pre-monsoon and monsoon seasons whereas underestimated during the post-monsoon and winter seasons. Moreover, the performance of TMPA in plain- and medium-elevated regions was better in comparison with high elevated regions.

Generally, in Pakistan, the literature demonstrated that TRMM (RT and Adj) and TMPA performance is better in plain and medium elevated areas, however, both the products overestimate the precipitation in mountainous and glacial regions in the north and coastal areas. Based on the studies conducted over Pakistan, it is concluded that the performance of different SPPs shows significant temporal (daily, monthly, and annual), seasonal (pre-monsoon, monsoon, and post-monsoon), precipitation intensities, climate, and geotopographic dependency. Most of the studies conducted in Pakistan evaluated the TRMM-TMPA, PERSIANN, PERSIANN-CDR, and CMORPH. However, GPM-IMERG is still to be evaluated against other SPPs in Pakistan.

The objectives of this study are twofold: (1) to evaluate the GPM-IMERG with previously evaluated SPPs in Pakistan such as TMPA_3B43 v7, PERSIANN, and PERSIANN-CDR based on climate and topographic diversity and seasonal precipitation variation, i.e., pre- and post-monsoon, monsoon and winter seasons and (2) to select best SPPs and propose an Ensemble Precipitation (EP) algorithm and its evaluation with the selected SPPs in Pakistan. Unlike many other studies available in the literature, a novelty in this study is the development of the EP algorithm by applying the paired sample *t*-test and principal component analysis (PCA) methods.

2. Materials and Methods

2.1. Study Area

Pakistan is situated geographically between 24° and 37°N latitude and 62° and 75°E longitude in the western zone of South Asia and covers approximately 79.6 million ha of the area (Figure 1). Pakistan has complex and diverse topography with elevation ranges from 0 m (Arabian sea) to the world famous Himalayas and Karakoram mountain ranges with a peak elevation of 8600 m [45]. The landscape diversity ranges from glacial and snow cover region in the north, to a plain zone having deserts and plateaus in the middle, and a coastal zone along the Arabian Sea in the south. Due to diverse climatic regimes, the annual precipitation of Pakistan ranges from 300 mm in the south to about 1500 mm in the north. The maximum precipitation occurs during summer (Monsoon) and winter (western disturbances) seasons [46]. Monsoon precipitation occurs during July to September and originates from the Bay of Bengal and enters Pakistan from east and northeast. During the monsoon season, heavy precipitation (from 55 to 60% of annual precipitation) is received in the country [47]. Winter precipitation occurs during December to March due to the Mediterranean Sea and enters Pakistan from Iran and Afghanistan. Moderate precipitation (30% of annual precipitation) is received during the Winter season [48].

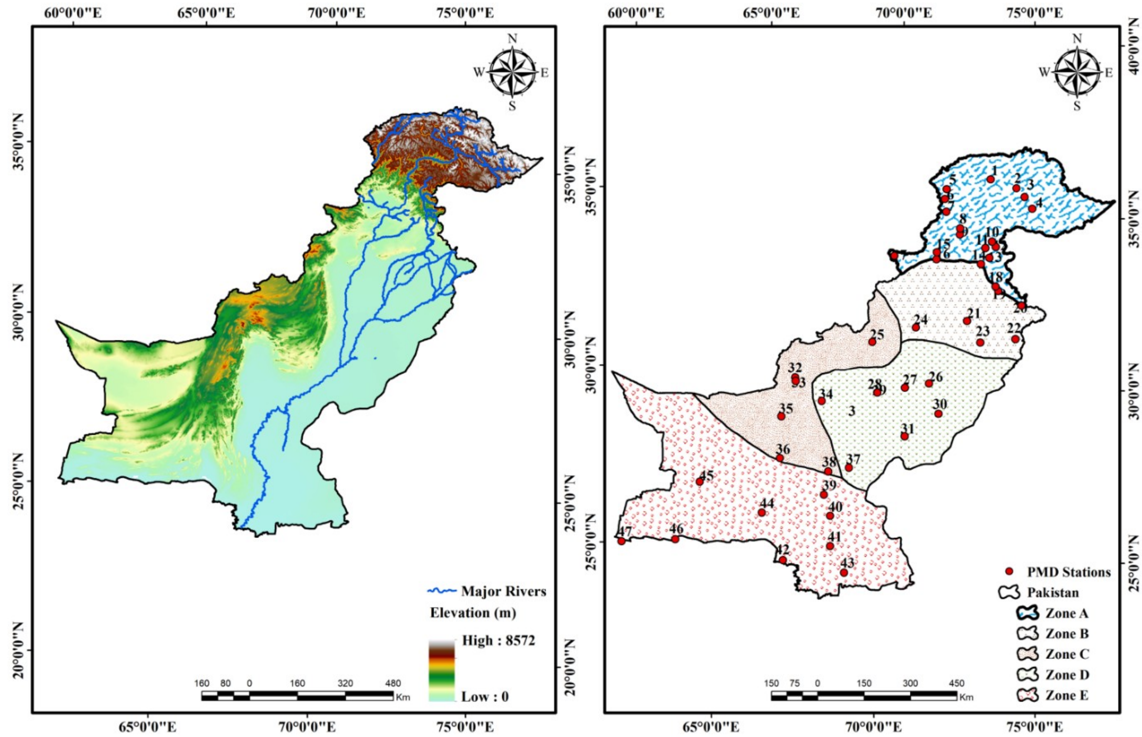

(**a**) (**b**)

Figure 1. (**a**) Elevation and major rivers of Pakistan. (**b**) Five climate zones of Pakistan and selected Pakistan Meteorological Department (PMD) surface precipitation gauges (SPGs) (the SPG numbers and associated SPG names are shown in Table 1).

The Indus River is the most important river in Pakistan. The Indus River originates from Mount Kailash in Tibet (China) and discharges into the Arabian Sea. The Indus River covers most of Khyber Pakhtunkhwa, Punjab and Sindh provinces of Pakistan, with the Himalayan mountains (North–East) and Highland regions in the north and the arid regions in the southwest. Salma et al. [49] divided Pakistan into five different microclimate zones (Figure 1).

2.2. In Situ Data

Surface Precipitation Gauges (SPGs) are considered as ground truth data, as they provide a direct record of the precipitation at a specific location. The SPP observations at the grid cell are compared with the corresponding SPG during the calibration and validation phases. To monitor the precipitation and climate variation in Pakistan, PMD has established a significant number of weather SPGs all over Pakistan, including some dating back to 1950, some seasonal ones, and some newly established ones. A total of 97 observatories are installed all over Pakistan on behalf of PMD. The precipitation data is collected manually which is subjected to human-induced and instrumental errors. Other associated errors with the SPG located at high elevation regions comes from wind effect, which affects the precipitation measurement by the SPGs. In these circumstances, PMD follows the World Meteorological Organization (WMO) standard code WMO-N for the evaluation and correction of SPG precipitation data to ensure the consistency in the measurements. In this research, daily precipitation data at 47 SPGs are obtained from PMD for the year 2015 and 2016. Table 1 shows the details of all the SPGs utilized in this study.

The dataset is divided into five different climate zones (Zone-A to Zone-E) for evaluation of the topographical and seasonal performance of SPPs. Zone-A is situated from 34°N to 38°N, has cold climate and high mountains like Hindukush, Himalaya, and Koh-e-Sufaid with mean annual precipitation (MAP) of 1034.43 mm. Zone-B lies between 31°N and 34°N and has a mild cold climate and submountains (MAP of 990.72 mm). Zone-C is located between 27°N and 32°N and has cold weather in winter and hot weather in summer (MAP of 317.00 mm). Zone-D is the hottest and arid zone of Pakistan. The area is almost plain in elevation with some area included in the famous Thar Desert (MAP of 322.41 mm). Zone-E is the coastal zone of Pakistan and situated near the Arabian Sea. The climate in this zone mostly ranges from arid to hyper-arid (MAP of 146.65 mm).

The zero-order method test is used to fill the missing data. The method employs a simple procedure by replacing the average for the missing values [50]. The data quality test is used to check the accuracy and consistency of the data. There are various statistical methods to test the quality of the data. It mainly contains the normality test such as the Jarque–Bera test, histogram (graphical approach), the mean, the skewness, and kurtosis of the data [51]. For the current study, the skewness and kurtosis method is applied to test the data quality.

2.3. Description of Satellite-Based Precipitation Datasets

Three different satellite-based precipitation datasets have been used in the present study. Which include the Integrated Multi-Satellite Retrievals for Global Precipitation Measurement (IMERG), Tropical Rainfall Measurement Mission (TRMM) Multi-satellite Precipitation Analysis (TMPA), and Precipitation Estimation from Remotely Sensed Information using Artificial Neural Networks (PERSIANN).

The IMERG is the quasi-global (between 60°N and 60° S) multi-satellite precipitation product of Global Precipitation Measurement (GPM) [52]. The GPM-IMERG mission was launched in February 2014 and has a spatial resolution of $0.1° \times 0.1°$ and a temporal resolution of 30 min. IMERG is the Level 3 precipitation algorithm of GPM, which has three runs, i.e., early run (latency of 6 h and can be used for warning a probable flood event or landslides), late run (latency of 18 h and suitable for drought monitoring and agricultural forecasting), and final run (latency of three months and used for observation like precipitation observation). In this study, IMERG final run will be used to estimate the seasonal and topographical variation of precipitation in Pakistan.

Tropical Rainfall Measurement Mission (TRMM) is the first space-borne SPP launched in November 1997 its detailed description is available in previous literatures [53–55]. TRMM has three onboard instruments, Precipitation Radar (PR), TRMM Microwave Image (TMI), and Visible Infrared Scanner (VIRS) for recording the data. TMI is a multichannel passive microwave radiometer that supplements the PR by providing total hydrometeor (liquid and ice) contents, with the precipitation systems. The VIRS dispensed the cloud context of precipitation structures and used to connect microwave precipitation information to infrared-based precipitation estimates from geosynchronous satellites [53–55]. Currently, the Multi-satellite Precipitation Analysis (TMPA) is producing the best precipitation estimates at 0.25° spatial resolution for the areas between 50°S and 50°N. The TMPA algorithm combines the precipitation estimates from various satellite systems, as well as SPG precipitation analyses [17,56]. TRMM TMPA-3B43 v7, a daily precipitation product, is used in this study.

The PERSIANN is an algorithm developed by the Center for Hydrometeorology and Remote Sensing (CHRS) in the University of California Irvine with a spatial resolution of $0.25° \times 0.25°$. In PERSIANN PMW data (TMI, AMSU-B, and SSM/I) is used to adjust the neural network parameters to increase precipitation estimation accuracy. PERSIAN–CDR is another product from PERSIANN family developed by CHRS with the spatial resolution of $0.25° \times 0.25°$. PERSIANN–CDR uses the same neural network for precipitation estimation as used previously but differs regarding input IR dataset with the use of GridSat-B1 instead of CPC-IR. Moreover, PMWs data are not used [57]. In this study, PERSIANN and PERSIANN-CDR algorithms are evaluated based on seasonal and regional scales.

Table 1. PMD SPGs used in the study along with SPG number (shown in Figure 1b), Latitude (N), Longitude (E), and Elevation (m).

SPG Number	SPG	Latitude (°)	Longitude (°)	Elevation (m)	SPG Number	SPG	Latitude (°)	Longitude (°)	Elevation (m)
1	Gupis	36.17	73.40	2156.00	26	Multan	30.20	71.43	122.00
2	Gilgit	35.92	74.33	1468.00	27	D.G.Khan	30.05	70.63	148.00
3	Bunji	35.67	74.63	1372.00	28	Chhor	29.80	69.70	5.00
4	Astore	35.37	74.90	490.43	29	Barkhan	29.88	69.72	1097.00
5	Chitral	35.85	71.83	1498.00	30	Bahawal Pur	29.39	71.68	110.00
6	Drosh	35.57	71.78	1464.00	31	Khanpur	28.80	70.40	89.00
7	Dir	35.20	71.85	1375.00	32	Quetta	30.18	66.95	1719.00
8	Saidu Sharif	34.73	72.35	961.00	33	Quetta (Samungli)	30.08	66.97	1626.00
9	Balakot	34.55	72.35	1528.35	34	Sibi	29.55	67.88	133.00
10	Muzaffarabad	34.37	73.48	838.00	35	Kalat	29.02	66.58	2015.00
11	Kakul	34.18	73.25	1308.00	36	Khuzdar	27.83	66.63	1231.00
12	Murree	33.92	73.38	2291.00	37	Rohri	27.67	68.90	66.00
13	Islamabad	33.58	73.09	507.00	38	Larkana	27.53	68.23	53.00
14	Garhi dupatta	34.22	73.62	814.00	39	Padidan	26.85	68.13	46.00
15	Peshawar	34.50	71.30	327.00	40	Nawab Shah	26.25	68.37	37.00
16	Cherat	33.82	71.89	1372.00	41	Hyderabad	25.38	68.41	28.00
17	Parachinar	33.86	70.08	1775.00	42	Karachi Airport	24.91	66.93	22.00
18	Mangla	33.07	73.63	284.00	43	Badin	24.63	68.90	9.00
19	Jhelum	32.90	73.30	288.00	44	Lasbella	26.23	66.17	87.00
20	Sialkot	32.50	74.50	255.00	45	Panjgur	26.97	64.10	968.00
21	Sarghoda	32.10	72.60	187.00	46	Pasni	25.27	63.48	9.00
22	Lahore PBO	31.60	74.40	216.00	47	Jiwani	25.07	61.80	56.00
23	Faisal Abad	31.34	73.13	185.00					
24	D.I.Khan	31.80	70.60	173.00					
25	Zhob	31.35	69.47	1405.00					

2.4. Adjustments in Spatial and Temporal Resolutions

All of the SPPs used in this study differ in spatial and temporal resolutions. To adjust the spatial resolution, an aggregation method was used to aggregate the precipitation product of IMERG from 0.1° to 0.25°, and the areal aggregation weights of 0.16, 0.08, and 0.04 were assigned to four IMERG grid cells falling inside a 0.25° TRMM grid cell, four located halfway within, and the ninth covers one-fourth inside, respectively [40]. Furthermore, the coordinate matching process was also performed to avoid any mismatch issue. In the coordinate matching process, the precipitation record and the latitude/longitude of the SPGs are matched against the amount of satellite precipitation in the pixel. To produce a single mean value at each pixel, the precipitation data is averaged when a pixel has more than one SPG.

The day in Pakistan begins 5 h ahead of Greenwich Mean Time (GMT+5). The satellite-based data accumulations are computed from 3:00 to 3:00 UTC to match the 8:00 to 8:00 local time of the SPG data in Pakistan. In order to compare the SPPs estimates with the SPGs data, the satellite precipitation data is accumulated into daily precipitation, which has the same temporal resolution as the SPG precipitation data.

2.5. Precipitation Products Evaluation

The selected four SPPs are quantitatively evaluated by comparing the SPPs with the daily PMD SPG observations from January 2015 to December 2016. The statistical indices used to assess the efficacy of selected SPPs are listed in Table 2, including (i) Mean Error (ME) to evaluate the bias, (ii) Root Mean Square Error (RMSE) to evaluate the magnitude of error with more emphasis on large errors as compared to ME, and (iii) the Pearson correlation coefficient (CC). For comprehensive evaluation of CC, the CC ranges mentioned by Iqbal and Athar [10] are considered: Weak (CC < 0.25), Low (0.25 < CC < 0.5), Moderate (0.5 < CC < 0.75), and Strong (0.75 < CC < 1).

Table 2. List of metrics used in statistical performance measures [a].

Statistical Measures	Equation	Perfect Value
Mean Error (ME)	$\frac{1}{n}\sum_{i=1}^{n}(X_i - Y_i)$	0
Root Mean Square Error (RMSE)	$\sqrt{\frac{1}{n}\sum_{i=1}^{n}(X_i - Y_i)^2}$	0
Correlation Coefficient (CC)	$\frac{\sum_{i=1}^{n}(X_i-\overline{X})(Y_i-\overline{Y})}{\sqrt{\sum_{i=1}^{n}(X_i-\overline{X})^2}\sqrt{\sum_{i=1}^{n}(Y_i-\overline{Y})^2}}$	1
Probability of Detection (POD)	$\frac{hit}{hit+miss}$	1
False Alarm Ratio (FAR)	$\frac{false\_alarm}{hit+false\_alarm}$	0
Critical Success Index (CSI)	$\frac{hit}{hit+miss+false\_alarm}$	1

[a] X_i and Y_i represents SPP- and SPG-based precipitation observations for the ith time step, respectively, $\overline{X}$ and $\overline{Y}$ are the average values of SPP- and SPG-based observations, n represents the sample size, *hit* is the number of events when the precipitation is recorded both by SPPs and SPGs, *miss* is the number of events missed by SPP and recorded by SPG observations, *false_alarm* is the number of events that SPP capture the precipitation while SPGs show no precipitation record.

For more accurate quantification of errors, three additional categorical statistical indices, including Probability of Detection (POD), False Alarm Ratio (FAR), and Critical Success Index (CSI), are used to detect the agreement between SPP- and SPG-based precipitation data. POD indicates how well the SPPs detect the precipitation events among all the SPG-based precipitation events (1 mm was used as the precipitation/no precipitation threshold [22], FAR indicates the fraction of incorrectly detected precipitation events by SPPs, and CSI represents an overall fraction of precipitation events correctly detected by the SPPs.

2.6. Algorithm for Ensemble Precipitation Estimation

The proposed algorithm for satellite-based ensemble precipitation estimation is based on K-fold cross-validation, paired sample *t*-test, Principal Component Analysis (PCA), and the ensemble algorithm.

The K-fold cross-validation method is used to evaluate the SPPs performance and its selection. In the K-fold cross-validation, the SPG observations in the five different climate zones are divided into K-datasets. Furthermore, these datasets are partitioned into training and testing sets. During the validation process, the data of a single SPG (testing set) in a selected climate zone is taken out from the calibration dataset (training set). The average error across all K-trials was calculated. The K-fold test was repeated for all the SPGs considered in the study.

A dependent-sample *t*-test, also known as paired sample *t*-test, is used to compare the SPPs with the SPG datasets. The paired sample *t*-test assesses whether the mean difference between paired objects/observations is significantly different from zero. The following two hypotheses are tested for the paired sample *t*-test.

Hypothesis 1. *Null Hypothesis*:

$$\mathrm{H}_0 : \mu_1 = \mu_2 \tag{1}$$

Hypothesis 2. *Alternative (Nondirectional) Hypothesis*:

$$\mathrm{H}_a : \mu_1 \neq \mu_2 \tag{2}$$

Hypothesis 3. *Alternative (Directional) Hypothesis*:

$$\mathrm{H}_a : \mu_1 < \mu_2 \text{ or } \mathrm{H}_a : \mu_1 > \mu_2 \tag{3}$$

where μ_1 and μ_2 are the mean of first and second variables. Moreover, the Wilcoxon matched-paired signed ranks test is also performed to examine the extreme violation of normality assumptions and further validation of the performance of SPPs. The mean error and standard deviation between the SPP and SPG datasets are calculated. Based on K-fold cross-validation and paired sample *t*-test with 95% confidence interval, the best satellite products (minimum mean error and standard deviation) are selected.

The Principal Component Analysis (PCA) technique uses a sophisticated mathematical principle to transform a number of possibly correlated variables into a smaller number of variables called principal components. The basic idea behind the application of PCA is to select the two best SPPs out of the four SPPs and to determine the percentage correlation of the selected SPPs with the ground truth data (PMD SPGs). This percentage is considered as a weight factor "*w*" ($\Sigma w = 1$) of the particular satellite product.

After calculating the weights, the precipitation observations of the selected SPPs over each climate zone have been combined using the following equation:

$$\mathrm{EP_i} = \mathrm{w_1 S_i} + \mathrm{w_2 s_i},\ i = 1, 2, \ldots, N \tag{4}$$

where EP is the ensemble precipitation, $\mathrm{w_1}$ and $\mathrm{w_2}$ are weights associated of the selected two SPPs, *S* and *s* are the two selected satellite products, *i* is the number of PMD SPGs, and *N* is the maximum number of SPP records in the particular climate zone.

Finally, the developed ensemble precipitation product EP = [EP_1, EP_2, ... , EP_N] is compared and evaluated with the corresponding ground observations G = [G_1, G_2, ... , G_N] using the statistical metrics presented in Table 2.

3. Results

The results obtained are divided into the following three sections. Section 3.1 describes the regional evaluation of IMERG, TMPA, PERSIANN, and PERSIANN-CDR, Section 3.2 describes the evaluation of ensemble precipitation (EP) algorithm, and Section 3.3 describes the validation of satellite products and EP algorithm on seasonal scales.

3.1. Regional Evaluation of Satellite Products

Accurate estimation of precipitation distribution is a challenging task over the mountainous region because of high precipitation variability due to the orographic enhancement and terrain-induced errors on remote sensing retrievals. The northern regions of Pakistan also pose uncertainties in precipitation estimation due to complex climatology and terrain of the region. Therefore, this research is conducted to test the abilities of IMERG over the complex topography of Pakistan by comparing with other SPPs (TMPA, PERSIANN, and PERSIANN-CDR) and against the SPG data. The regional performance of all the SPPs is evaluated on the annual temporal scale at different climate regions using statistical metrics listed in Table 2. The regional variability of all these metrics for IMERG, TMPA, PERSIANN, and PERSIANN-CDR over the selected five climatic regions is shown in Figure 2.

The ME results (Figure 2a) indicated that all the SPPs performed poorly in Zone-A (considerable overestimation of precipitation except at Parachinar SPG) as compared to the other zones. This error may be associated with the fact that in the glacial region, the presence of ice cover and cold cloud contribute to the overestimation [58,59]. Generally, the magnitude of ME shows a decreasing trend from North to South of the country. All the satellite performed well in Zone-E (slight underestimation) which is coastline area with relatively low elevation and rainfall intensity. Moreover, the performance of all SPPs is good in the Zone-C and Zone-B while moderate in Zone-D. Among all the SPPs, IMERG product showed significantly improved performance followed by TMPA. Higher ME (ME > 40 mm/month) is observed over Murree, Muzaffarabad, Dir, Drosh, etc., while smallest ME is observed at Jiwani and Badin SPGs.

Figure 2b indicates that RMSE is showing a similar trend to ME: higher RMSE at Zone-A and lower RMSE at low altitude climate zones. However, the RMSE of Zone-D is slightly higher compared to Zone-C and Zone-D. Maximum RMSE is observed at Drosh, Dir, and Balakot while minimum RMSE is observed at Larkana and Panjgur SPGs. Considering the Zone-D (a special scenario), maximum RMSE is observed at SPGs namely Khanpur and Bahawalpur, revealing the poor performance of satellite SPPs at those SPGs. Similar observations are found in the study conducted by Yawar [43], where RMSE is decreasing from North to South. The maximum RMSE associated to IMERG is 29.23 mm/month at Drosh SPG, while for TMPA the maximum RMSE is 38.50 mm/month at Dir SPG. For PERSIANN and PERSIANN-CDR maximum RMSE is observed Dir (65.14 mm/month) and Balakot (55.9 mm/month), respectively.

The performance evaluation based on CC (Figure 2c) revealed that IMERG agreed well with the majority of SPG observations as compared to TMPA, PERSIANN, and PERSIAN-CDR. The results revealed that IMERG performance is good over the Zones-B, C, and D, and average performance over Zone-A and Zone-E. IMERG shows high correlation with Bahawalpur SPG in Zone-D followed by Karachi airport (Zone-E), and Faisalabad (Zone-B) while relatively poor performance at Lasbella (Zone-E) and Sialkot (Zone-B) SPGs. However, TMPA has a high correlation with Khanpur (Zone-D), Faisalabad (Zone-B), and Karachi airport (Zone-E) SPGs while lower performance in Lasbella (Zone-E), Sialkot (Zone-B), and Dir (Zone-A). Overall, the results indicated that the performance of IMERG outperformed all other satellites over most of the SPGs.

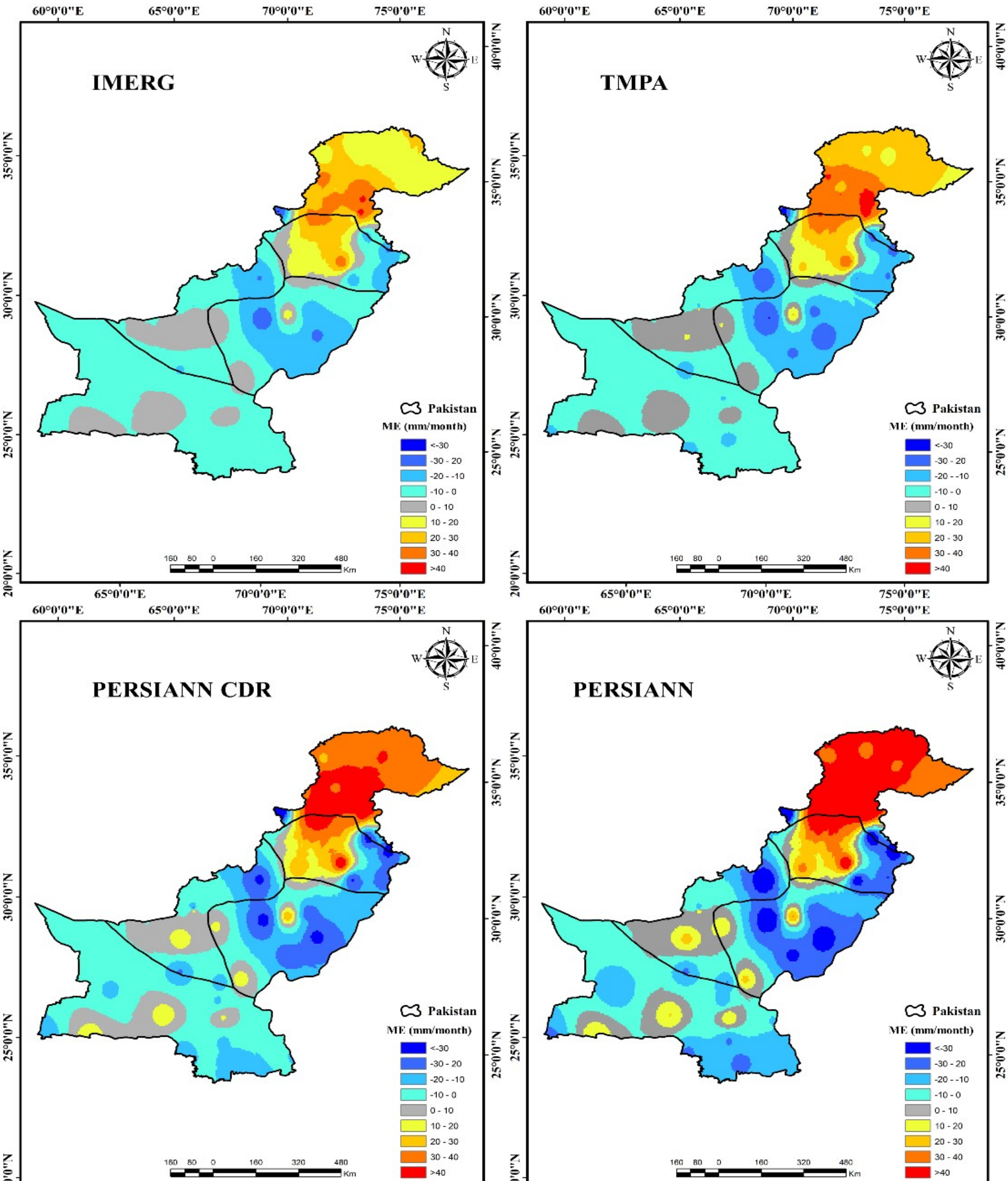

(**a**)

Figure 2. *Cont*.

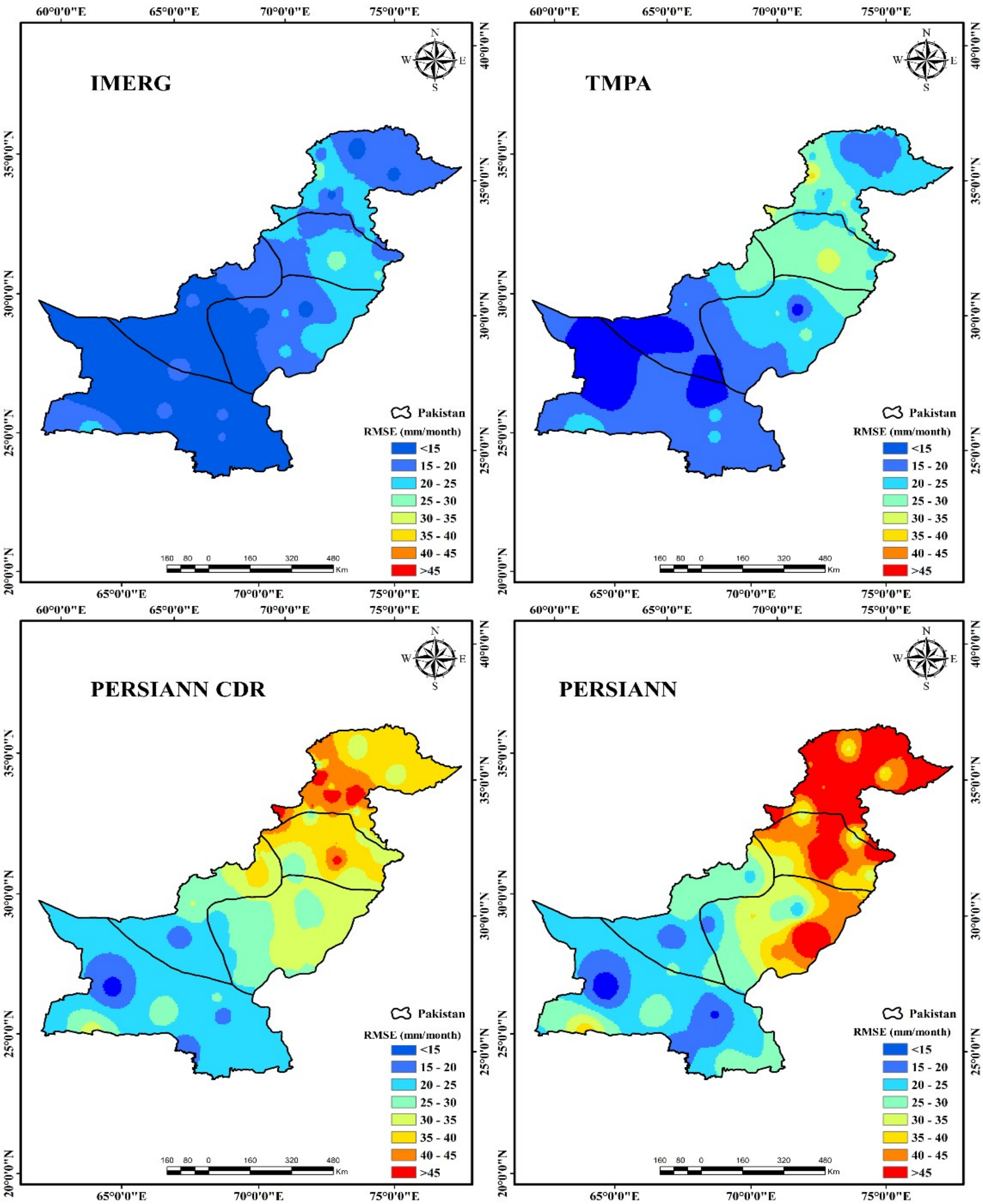

(**b**)

Figure 2. *Cont.*

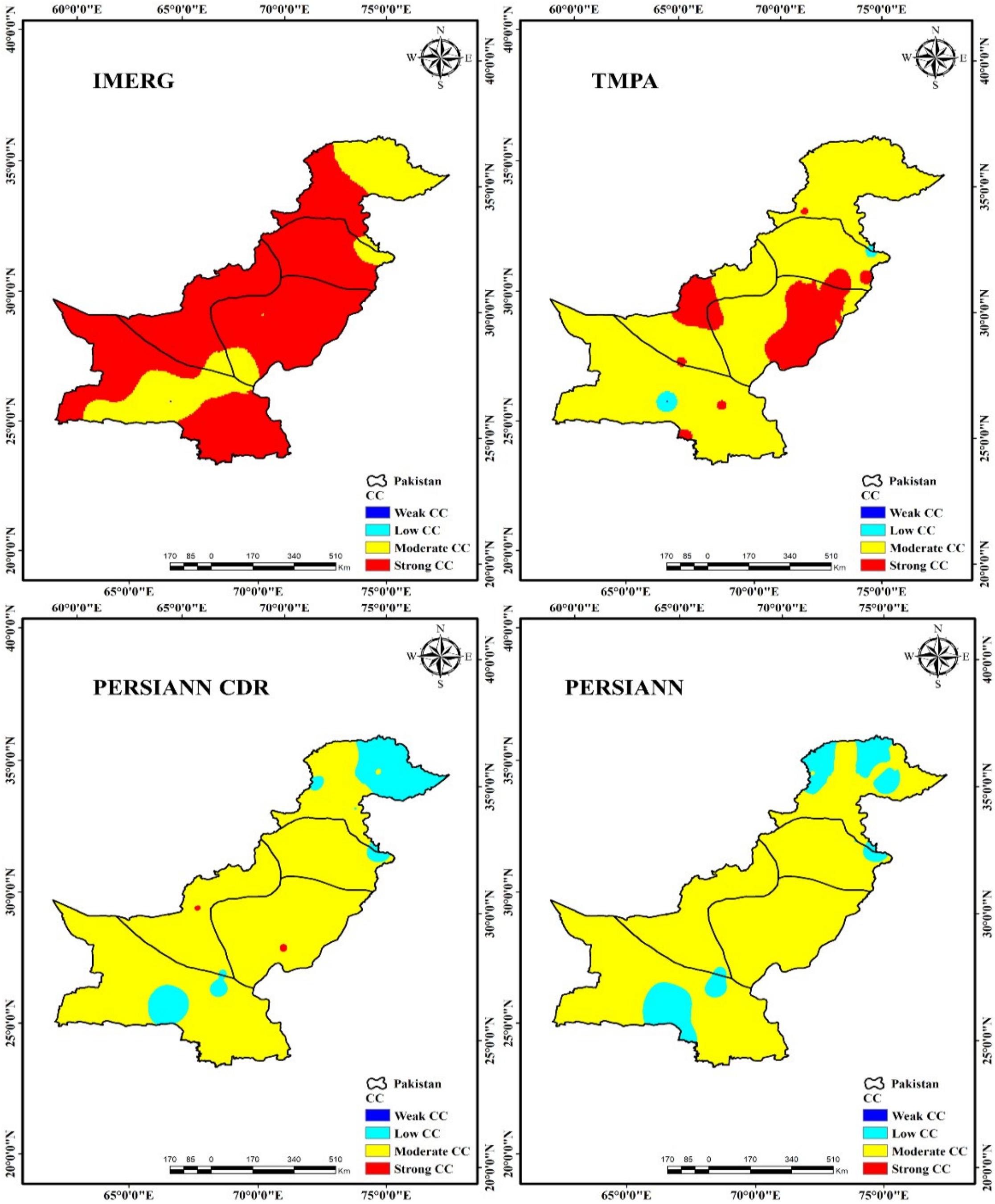

(**c**)

Figure 2. *Cont*.

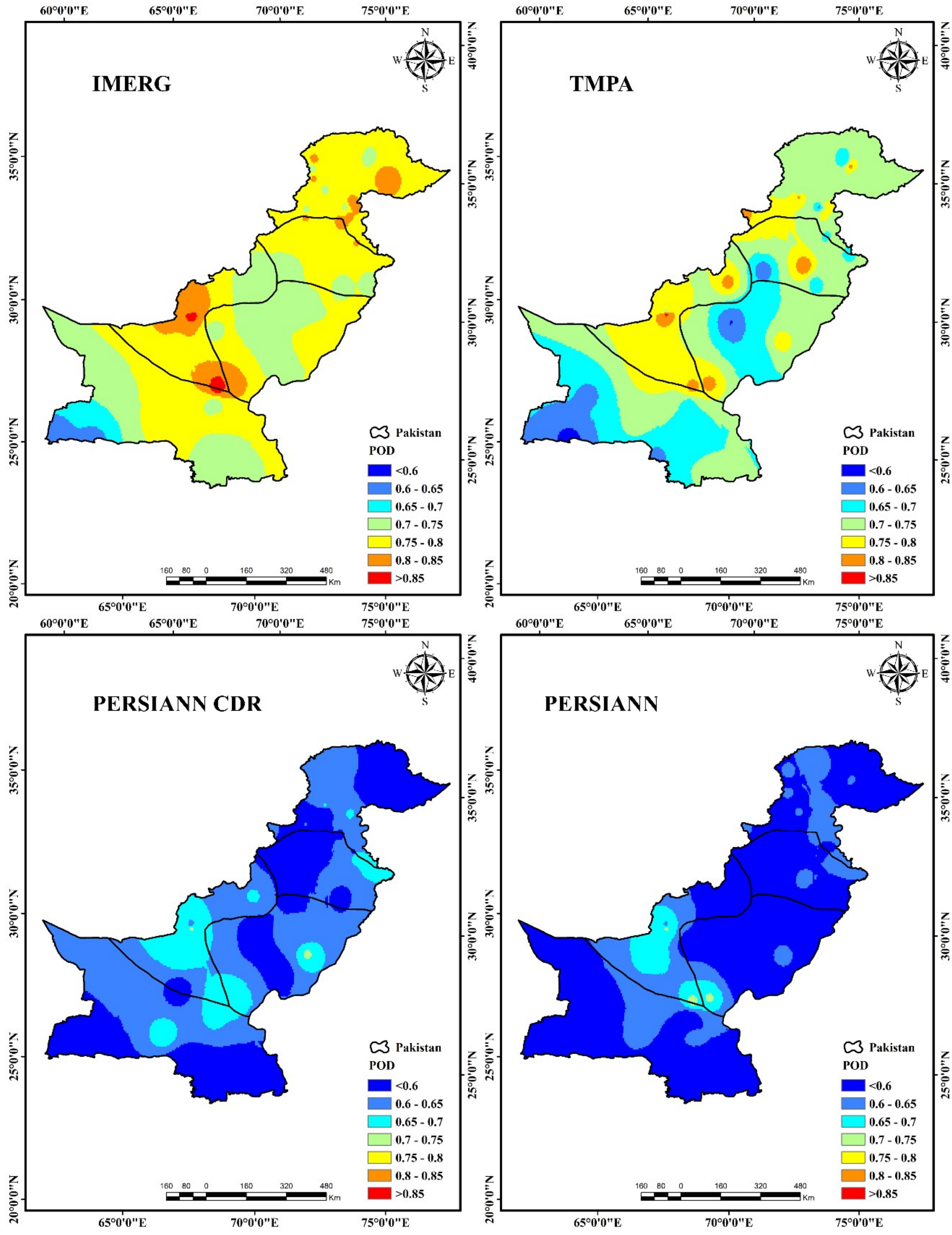

(**d**)

Figure 2. *Cont.*

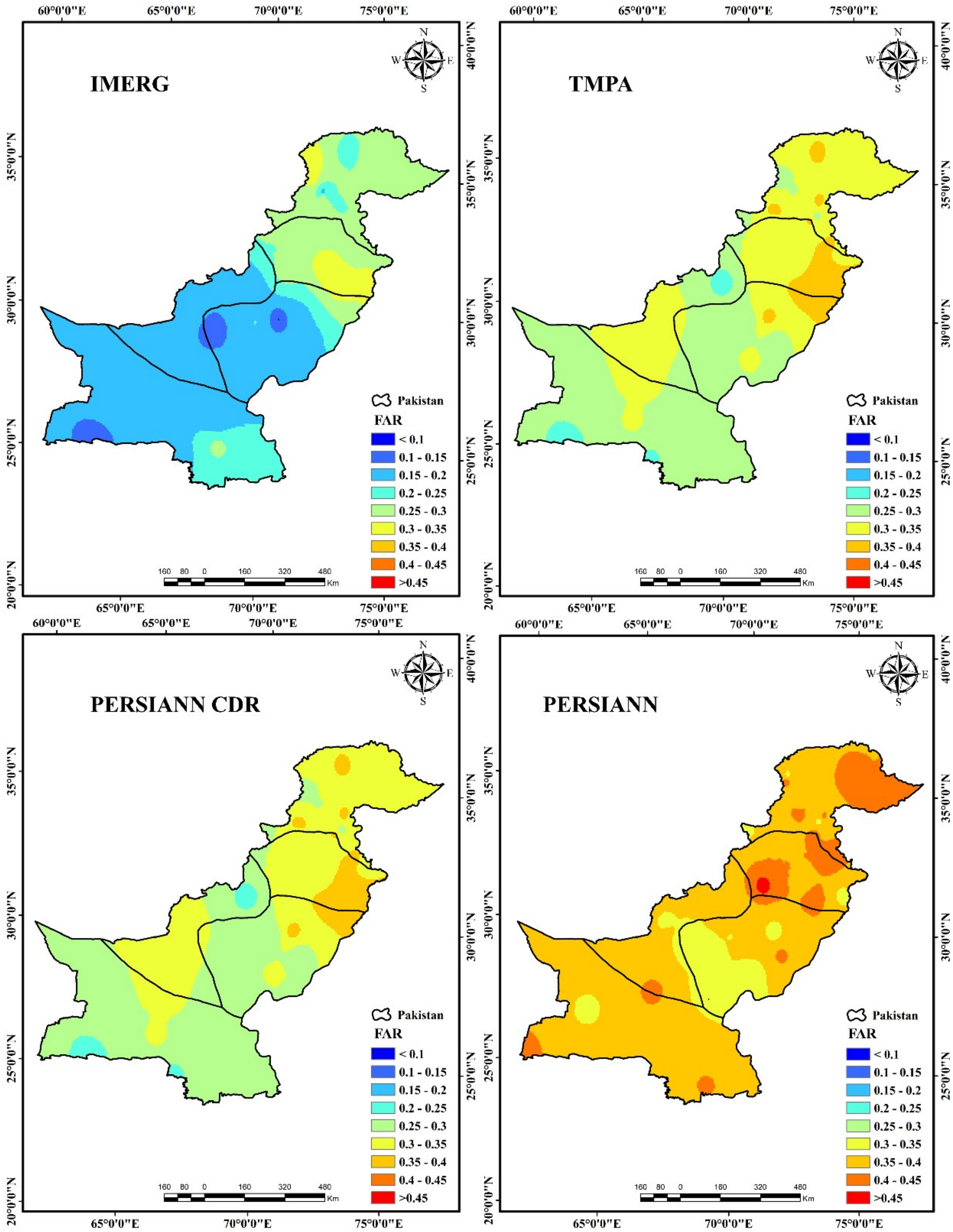

(e)

Figure 2. (**a**) Regional distribution of mean error (ME) of satellites precipitation estimates. (**b**) Regional distribution of RMSE of satellite precipitation estimates. (**c**) Regional distribution of CC of satellite precipitation estimates. (**d**) Regional distribution of POD of satellite precipitation estimates. (**e**) Regional distribution of FAR of satellite precipitation estimates.

Figure 2d,e shows the POD and FAR (evaluated on daily time scale) of all the satellite SPPs, respectively. The POD of IMERG and TMPA are significantly comparable over most of the SPGs in all the climate zones; whereas, the POD of PERSIANN and PERSIANN-CDR is slightly lower over most of the SPGs. However, FAR distribution of all the precipitation products is completely different from each other. In the case of IMERG, lower FAR values are observed over the plain regions as compared to TMPA. The CSI of all the precipitation products exhibits almost the similar trend, and the zone-based details are presented in Table 3.

Table 3. The average CSI of SPPs over the five climate zones.

SPPs	Zone-A	Zone-B	Zone-C	Zone-D	Zone-E
	Critical Success Index (CSI)				
IMERG	0.28	0.34	0.30	0.37	0.30
TMPA	0.23	0.27	0.24	0.28	0.26
PERSIANN	0.17	0.23	0.21	0.24	0.22
PERSIANN-CDR	0.21	0.23	0.22	0.26	0.22

Overall, the results presented that all the SPPs show the elevation dependencies which are characterized by overestimation at higher and slight/moderate underestimation over lower altitude regions. The IMERG performed best followed by TMPA at the majority SPGs in all zones. Furthermore, the SPPs are evaluated with regional SPGs, and high correlations of IMERG and TMPA with SPG observations are found. The performance of PERSIANN and PERSIANN CDR is found relatively poor as compared to IMERG and TMPA.

3.2. Ensemble Precipitation (EP) Algorithm Evaluation

Tables 4 and 5 show the paired sample *t*-test and PCA results, respectively. The paired sample *t*-test result shows the lowest mean error and standard deviation between the PMD and IMERG, followed by PMD and TMPA. This lowest mean error and the standard deviation are taken under consideration for EP algorithm which represent higher correlation between the compared pairs. The standard deviation and mean error of PMD-IMERG and PMD-TMPA is considerably low as compared to PMD-PERSIANN and PMD-PERSIANN CDR. Based on the high correlation, low standard deviation and mean error, IMERG, and TMPA satellite products are selected for the EP algorithm. The results of PCA, shown in Table 5, shows that the high correlation was found between the PMD-IMERG (61.82%) and PMD-TMPA (23.83%). Since the PERSIANN and PERSIANN CDR satellite products' performance was not satisfactory, their percentages and associated weights are distributed among the IMERG and TMPA for the final EP algorithm. The final weights for IMERG and TMPA are calculated by linear correlation, and the magnitude is 0.71 and 0.29, respectively.

Table 4. Paired sample *t*-test of satellite products over the five climate zones.

Pairs	Mean	Standard Deviation	Standard Mean Error	95% Confidence Interval of the Difference	
				Lower	Upper
PMD-IMERG	1.26	13.83	2.02	−2.80	5.32
PMD-TMPA	2.99	18.92	2.76	−2.55	8.55
PMD-PERSIANN	10.93	29.92	4.36	2.14	19.71
PMD–PERSIANN CDR	2.31	27.05	3.94	−5.63	10.25

Table 5. Principal component analysis (PCA) of satellite products over the five climate zones.

Satellite Products	Eigenvalues	Percentage Contribution	Percentage Weight
IMERG	2.47	61.82	0.62
TMPA	0.86	23.83	0.24
PERSIANN	0.20	5.18	0.05
PERSIANN CDR	0.44	9.17	0.09

The developed EP algorithm framework was evaluated using the same statistical metrics presented in Table 2. Table 6 shows the complete details of the Statistical Metrics for the EP algorithm at all the PMD SPGs. The result (Table 6 and Figure 3) indicated that ME and RMSE are significantly decreased while CC increased at most of the SPGs as compared to IMERG, TMPA, PERSIANN, and PERSIANN-CDR. However, some of the SPGs such as Cherat, Garhi Dupatta, Kakul, and Muzaffarabad still have higher ME and RMSE.

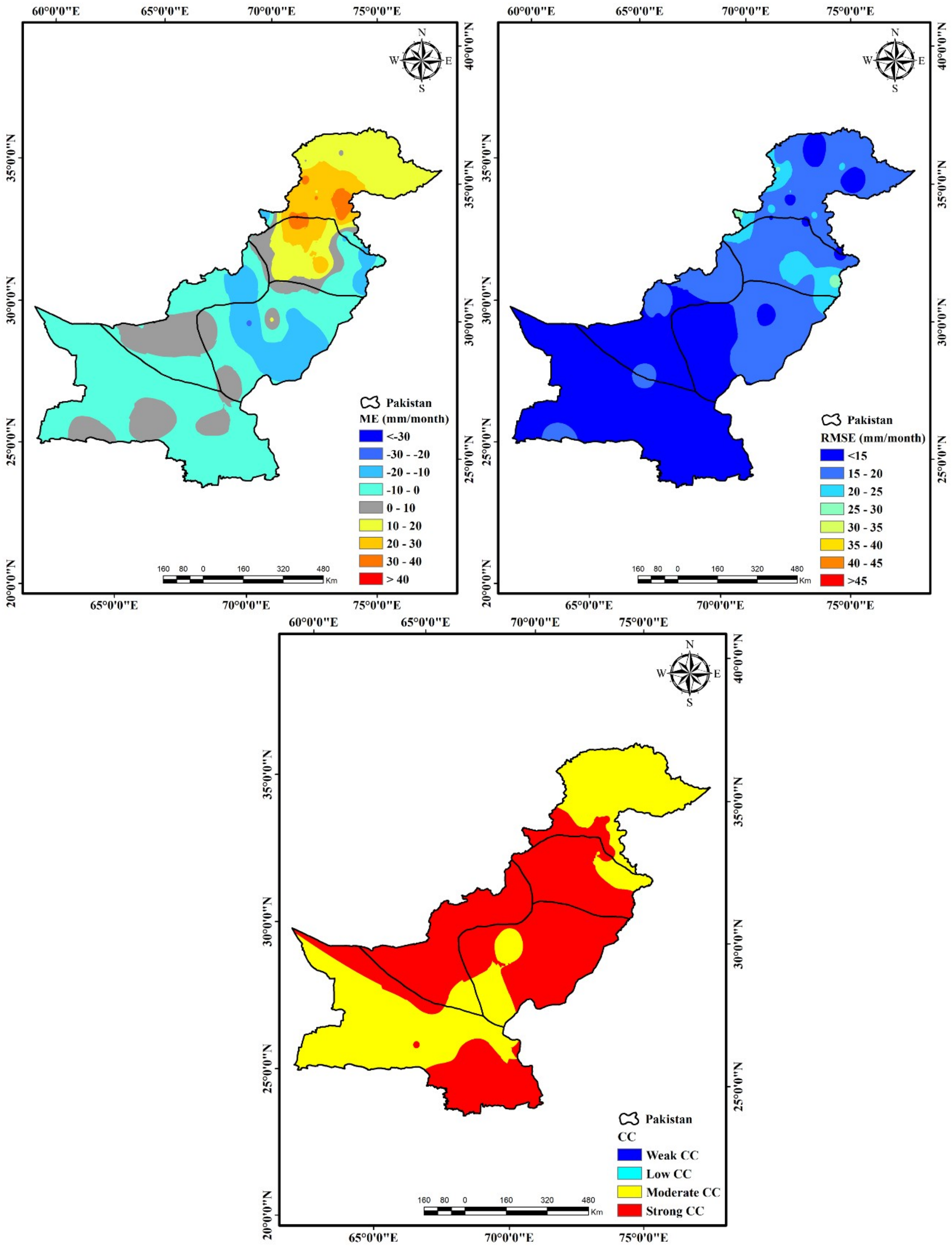

Figure 3. EP algorithm evaluation.

Table 6. Statistical evaluation of ensemble precipitation (EP) algorithm at selected SPGs.

SPG	ME (mm/month)	RMSE (mm/month)	CC	SPG	ME (mm/month)	RMSE (mm/month)	CC
Badin	−4.29	9.06	0.91	Kakul	29.89	19.58	0.82
Chhor	−21.71	12.86	0.82	Kalat	5.73	8.19	0.92
Hyderabad	−1.15	11.86	0.82	Khanpur	−14.61	18.49	0.87
Karachi Airport	−5.69	9.75	0.91	Khuzdar	−9.84	19.31	0.91
Astore	18.34	9.60	0.78	Lasbella	5.01	7.11	0.62
Balakot	31.66	9.28	0.84	Muzaffarabad	39.95	20.00	0.87
Cherat	39.86	13.80	0.82	Nawab Shah	4.58	8.33	0.87
Chitral	9.44	18.07	0.84	Padidan	−5.29	9.35	0.65
Dir	33.79	23.12	0.84	Panjgur	−3.68	4.99	0.82
Drosh	19.95	26.49	0.82	Parachinar	−19.18	26.11	0.77
Faisal Abad	−9.74	19.42	0.91	Pasni	3.51	18.45	0.77
Garhi Dupatta	32.93	19.27	0.82	Peshawar	24.46	22.27	0.87
Gilgit	12.40	18.20	0.72	Quetta	−9.12	18.83	0.92
Gopis	9.46	9.40	0.83	Rohri	6.49	9.38	0.72
Jhelum	−8.70	19.82	0.72	Sarghoda	29.12	23.51	0.82
Lahore PBO	−15.56	26.23	0.91	Sibi	7.47	13.67	0.82
Multan	−12.90	12.17	0.91	Zhob	−19.34	19.18	0.77
Murree	39.73	21.40	0.81	D.G.Khan	11.01	19.52	0.82
Saidu Sharif	18.51	20.76	0.82	Larkana	−2.25	3.37	0.72
Sialkot	−18.70	13.03	0.62	Mangla	−13.79	16.75	0.82
Bahawal Pur	−18.94	19.74	0.91	Quetta (Samungli)	8.73	13.10	0.92
Barkhan	−19.09	9.64	0.77				
Bunji	15.44	21.51	0.72	**Maximum**	39.95	26.49	0.92
D.I.Khan	16.84	18.29	0.91	**Median**	5.01	18.07	0.82
Islamabad	13.50	12.02	0.82	**Mean**	5.32	15.69	0.82
Jiwani	−5.59	13.35	0.72	**Minimum**	−21.71	3.37	0.62

3.3. Seasonal Evaluation of Satellite Products and EP Algorithm

The selected SPPs, i.e., IMERG, TMPA, and EP algorithm, were evaluated for the four seasons: pre-monsoon (April, May, and June), monsoon (July, August, and September), post-monsoon (October and November), and winter (December, January, February, and March) over Pakistan. Pakistan receives a higher percentage (60%) of precipitation during the Monsoon season (July to September). The monsoon precipitation varies spatially in magnitude from low (around 100 mm) in the south (24–28°N), higher (>700 mm) in the northeast (29–33°N), and again low (<100 mm) in the far north (glacial region, 34–36°N) [11].

Figure 4 shows the average precipitation where PMD and SPG records are compared with the selected SPPs and developed EP algorithm over the five climate zones in the four seasons. The figure shows that high precipitation is received in the monsoon season followed by the pre-monsoon season. Zone A receive high precipitation, and a decreasing trend is observed as we go toward the south. During the pre-monsoon season, IMERGE significantly overestimated the precipitation in Zone-E. While it significantly underestimated it in Zone-C. Contrarily, TMPA overestimated the precipitation over all the climate zones except Zone-C. However, the EP algorithm showed a better performance in plain areas while promising performance in elevated zones.

Moreover, during the Monsoon season, IMERG closely predicted the precipitation in all the climate zones while TMPA highly overestimated the heavy precipitation in Zone-A and other plain areas and underestimated the precipitation in Zone-C. The EP algorithm slightly overestimated the precipitation in Zone-A while performed well in plain areas. In the post-monsoon season, both the IMERG and TMPA underestimated the precipitation across all the five climate zones except Zone-D and Zone-E. Moreover, EP algorithm closely predicted the precipitation in the plain area, however, overestimated the precipitation at elevated zones. While in the winter season, IMERG and TMPA underestimated the precipitation in all climate zones except Zone-E and Zone-C, respectively. On the other hand, the EP algorithm performed poorly in Zone-C while high performance is observed over other four climate regions. Overall, IMERG showed high performance in capturing heavy precipitation and relative lower performance in moderate/low precipitation seasons. The EP algorithm performed very well in plain areas irrespective of the season and showed relatively poor performance over mountainous regions. TMPA highly overestimated the heavy precipitation and underestimated the moderate/lower precipitation.

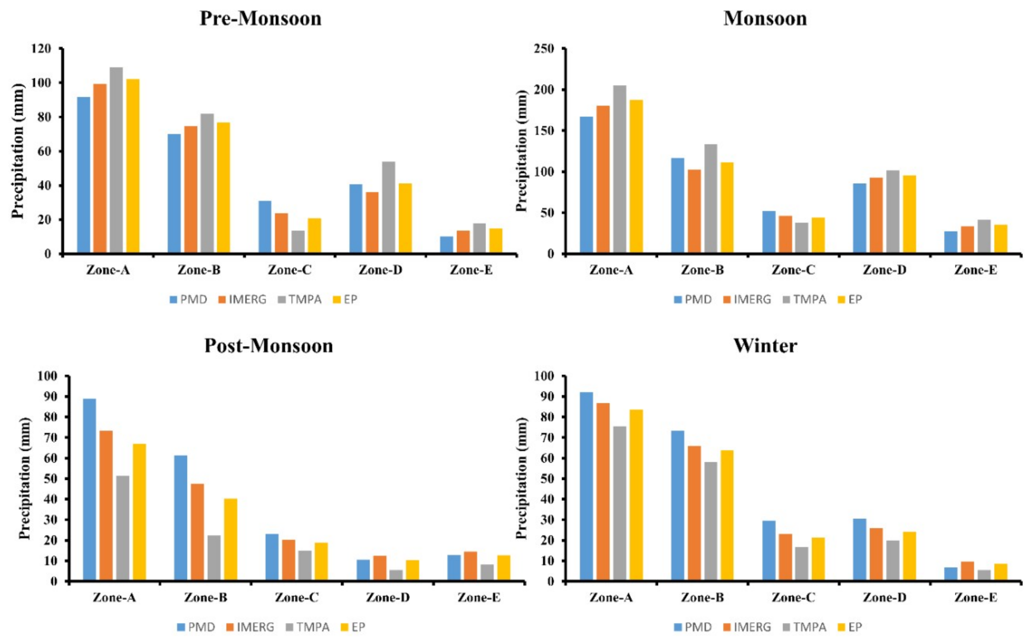

Figure 4. Comparison of mean seasonal (daily accumulated) precipitation over the five climate zones.

The mean error (ME) and root mean square error (RMSE) over the five zones compared to the PMD SPG data is shown in Figures 5 and 6, respectively. Figure 5 depicts that the IMERG, TMPA and EP algorithm overestimated the precipitation in pre-monsoon and monsoon seasons with the exception in Zone-D where IMERG and TMPA underestimate the precipitation. While they underestimated the precipitation in post-monsoon and winter. Based on the magnitude of the ME, the TMPA experienced a high error while the EP algorithm performed well in all the climate zones in every season. Figure 6 presents the magnitude of seasonal variation of RMSE of all the four seasons over the five climate zones. Higher RMSE is observed during the monsoon season followed by pre-monsoon. Generally, the performance of the EP algorithm and IMERG are reasonably well all over the seasons as compared to TMPA.

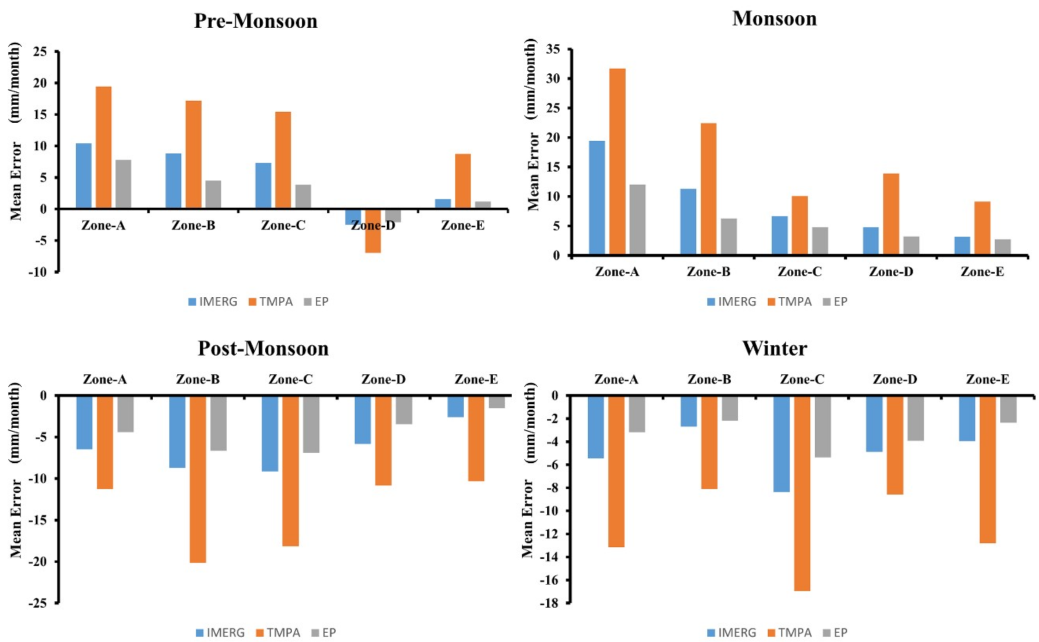

Figure 5. Mean error (ME) of satellite products and EP algorithm during the pre-monsoon, monsoon, post-monsoon and winter seasons.

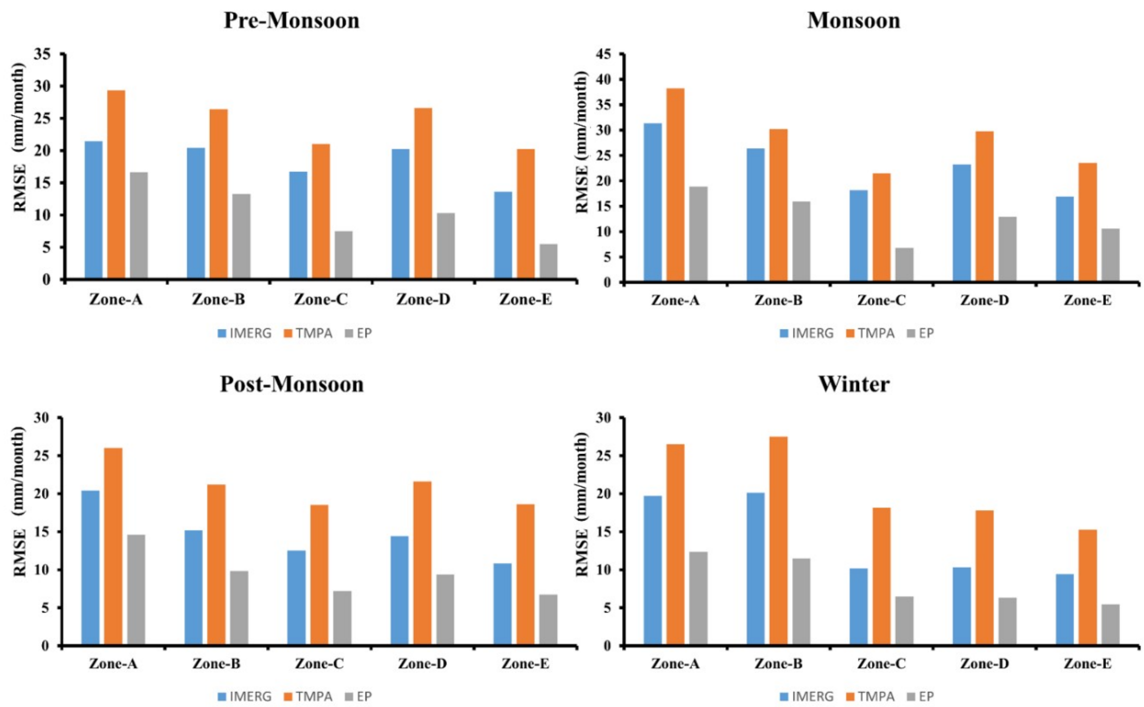

Figure 6. Root mean square error (RMSE) of satellite products and EP algorithm during the pre-monsoon, monsoon, post-monsoon, and winter seasons.

4. Discussion and Conclusions

Accurate estimation of precipitation with high spatial and temporal resolution is a very important for different hydrological simulations and climate change studies. Recently SPPs are attracting the attention of researchers and play a vital role in estimating precipitation in ungauged or poorly gauged regions. However, it is a challenging task in the developing countries such as Pakistan having sparse SPG network and complex topography. Based on the spatial (regional) scale evaluation (Figure 2a–e), our study supports the findings of previous literatures [10,43] conducted in Pakistan. In this study, it has been observed that high errors are found over high elevations, and these errors are reducing with the elevations from north to south. The IMERG and TMPA resulted in a poor performance at high elevated zone (Zone-A) of the study area. There could be number of reasons such as external error associated to the SPG (for example, wind effect, splashing effect of precipitation, evaporation from the SPGs and human-induced errors), complex topography, climate variability in the region, seasonality (pre-monsoon, monsoon, post-monsoon, and winter etc.) [10,13,39], and a sparse SPG network. However, a strong correlation has been observed over the plain elevation and low positive correlation over high elevation. These findings are consistent with the previous studies. However, the EP performed exceptionally well in plain areas while its performance is reducing with the elevation.

The IMERG and TMPA overestimated the precipitation during the pre-monsoon and monsoon seasons while underestimated the precipitation during post-monsoon and winter seasons. Moreover, good agreement between IMERG and SPGs was found in plain and medium elevated regions. These findings are consistent with the previous studies. However, EP performed very well during high and moderate precipitation while its performed ordinary in low precipitation events.

Different algorithms such as algorithms for improved calibration, reducing sampling issue, moving from TRMM to GPM, etc., have been implemented to reduce the non-negligible error in the SPPs. However, there is still room for further advancement in those algorithms to provide consistent results [14,40]. Effort has been made by Muhammad Waseem et al. [42] to minimize the inconsistency issues and the associated errors by merging different SPPs. Their algorithm is based on leave-one-out cross-validation (LOOCV), regional performance weights (MSE_r^j), and the ensemble algorithm. They concluded that their developed algorithm presented better agreement than the selected SPPs. In this study, we developed ensemble precipitation (EP) product for each SPG in the study area based on selecting two (best) out of four SPPs, i.e., IMERG and TMPA 3B43 v7. The best SPPs were selected using the paired sample *t*-test, and the corresponding weights are calculated using the principal component analysis (PCA). The developed EP algorithm was evaluated based on regional and temporal scales. The performance of the developed EP algorithm based on statistical evaluation is found comparatively better than the RP algorithm developed by Muhammad Waseem et al. [42]. Moreover, the EP algorithm has also been tested on a seasonal scale, and the algorithm performed well when evaluated by ME and RMSE. Overall, the developed EP algorithm performed very well across all the Pakistan irrespective of the seasons.

The EP algorithm is evaluated on spatial and temporal scales, and it has been observed that it outperformed the IMERG and TMPA in the plain and medium elevated areas. However, it performed relatively poorer over high elevated regions. The EP algorithm performed significantly better when evaluated based on temporal (seasonal) scale. Overall, the EP algorithm can capture the spatial precipitation pattern over the region at annual and seasonal scales very well. Moreover, the methodology presented in this study is very simple, and it has the capability to select the best SPPs for a specific region to minimize the errors associated SPPs to ensure consistency in the performance.

Author Contributions: U.R.K. and S.S. formulated the method; U.R.K. and S.M. analyzed the data; U.R.K. and S.S. interpreted the results; U.R.K. wrote the paper; and L.J. and S.M. provided the reviews and suggestions.

Funding: This research was partially supported by the National Natural Science Foundation of China (grant number 51479090).

Acknowledgments: The authors would like to acknowledge the Pakistan Meteorological Department (PMD) for providing the ground truth data and grateful to SPP datasets developers. The valuable comments from the editor and the two anonymous reviewers are greatly appreciated.

Conflicts of Interest: The authors declare no conflicts of interest.

References

1. Kidd, C.; Huffman, G. Global precipitation measurement. *Meteorol. Appl.* **2011**, *18*, 334–353. [CrossRef]
2. Ebert, E.E.; Janowiak, J.E.; Kidd, C. Comparison of near-real-time precipitation estimates from satellite observations and numerical models. *Bull. Am. Meteorol. Soc.* **2007**, *88*, 47–64. [CrossRef]
3. Guo, H.; Chen, S.; Bao, A.; Hu, J.; Gebregiorgis, A.S.; Xue, X.; Zhang, X. Inter-comparison of high-resolution satellite precipitation products over Central Asia. *Remote Sens.* **2015**, *7*, 7181–7211. [CrossRef]
4. Li, Z.; Yang, D.; Hong, Y. Multi-scale evaluation of high-resolution multi-sensor blended global precipitation products over the Yangtze River. *J. Hydrol.* **2013**, *500*, 157–169. [CrossRef]
5. Wu, H.; Adler, R.F.; Hong, Y.; Tian, Y.; Policelli, F. Evaluation of global flood detection using satellite-based rainfall and a hydrologic model. *J. Hydrometeorol.* **2012**, *13*, 1268–1284. [CrossRef]
6. Cohen Liechti, T.; Matos, G.D.S.C.; Pedro, J.; Boillat, J.-L.; Schleiss, A. Comparison and evaluation of satellite derived precipitation products for hydrological modeling of the Zambezi River Basin. *Hydrol. Earth Syst. Sci.* **2012**, *16*, 489–500. [CrossRef]
7. Tong, K.; Su, F.; Yang, D.; Hao, Z. Evaluation of satellite precipitation retrievals and their potential utilities in hydrologic modeling over the Tibetan Plateau. *J. Hydrol.* **2014**, *519*, 423–437. [CrossRef]
8. Moazami, S.; Golian, S.; Hong, Y.; Sheng, C.; Kavianpour, M.R. Comprehensive evaluation of four high-resolution satellite precipitation products under diverse climate conditions in Iran. *Hydrol. Sci. J.* **2016**, *61*, 420–440. [CrossRef]
9. Cheema, M.J.M.; Bastiaanssen, W.G. Local calibration of remotely sensed rainfall from the TRMM satellite for different periods and spatial scales in the Indus Basin. *Int. J. Remote Sens.* **2012**, *33*, 2603–2627. [CrossRef]
10. Iqbal, M.F.; Athar, H. Validation of satellite based precipitation over diverse topography of Pakistan. *Atmos. Res.* **2018**, *201*, 247–260. [CrossRef]
11. Khan, S.I.; Hong, Y.; Gourley, J.J.; Khattak, M.U.K.; Yong, B.; Vergara, H.J. Evaluation of three high-resolution satellite precipitation estimates: Potential for monsoon monitoring over Pakistan. *Adv. Space Res.* **2014**, *54*, 670–684. [CrossRef]

12. Raich, R.; Alpert, P.; Messer, H. Vertical precipitation estimation using microwave links in conjunction with weather radar. In Proceedings of the 15th International Conference on Environmental Science and Technology, Rhodes, Greece, 31 August–2 September 2017.
13. Tapiador, F.; Navarro, A.; Levizzani, V.; García-Ortega, E.; Huffman, G.; Kidd, C.; Kucera, P.; Kummerow, C.; Masunaga, H.; Petersen, W. Global precipitation measurements for validating climate models. *Atmos. Res.* **2017**, *197*, 1–20. [CrossRef]
14. Tang, G.; Ma, Y.; Long, D.; Zhong, L.; Hong, Y. Evaluation of GPM Day-1 IMERG and TMPA Version-7 legacy products over Mainland China at multiple spatiotemporal scales. *J. Hydrol.* **2016**, *533*, 152–167. [CrossRef]
15. Hartmann, D.; Klein Tank, A.; Rusticucci, M. Observations: Atmosphere and surface, chap. 2 in: Climate change 2013: The physical science basis. In *Contribution of Working Group I to the Fifth Assessment Report of the Intergovernmental Panel on Climate Change*; Cambridge University Press: Cambridge, UK; New York, NY, USA, 2013.
16. Munoz, E.A.; Di Paola, F.; Lanfri, M.A. Advances on rain rate retrieval from satellite platforms using artificial neural networks. *IEEE Lat. Am. Trans.* **2015**, *13*, 3179–3186. [CrossRef]
17. Huffman, G.J.; Bolvin, D.T.; Nelkin, E.J.; Wolff, D.B.; Adler, R.F.; Gu, G.; Hong, Y.; Bowman, K.P.; Stocker, E.F. The TRMM multisatellite precipitation analysis (TMPA): Quasi-global, multiyear, combined-sensor precipitation estimates at fine scales. *J. Hydrometeorol.* **2007**, *8*, 38–55. [CrossRef]
18. Casella, D.; Dietrich, S.; Di Paola, F.; Formenton, M.; Mugnai, A.; Porcù, F.; Sanò, P. PM-GCD-a combined IR-MW satellite technique for frequent retrieval of heavy precipitation. *Nat. Hazards Earth Syst. Sci.* **2012**, *12*, 231–240. [CrossRef]
19. Sorooshian, S.; Hsu, K.-L.; Gao, X.; Gupta, H.V.; Imam, B.; Braithwaite, D. Evaluation of PERSIANN system satellite–based estimates of tropical rainfall. *Bull. Am. Meteorol. Soc.* **2000**, *81*, 2035–2046. [CrossRef]
20. Zhu, H.; Li, Y.; Huang, Y.; Li, Y.; Hou, C.; Shi, X. Evaluation and hydrological application of satellite-based precipitation datasets in driving hydrological models over the Huifa river basin in Northeast China. *Atmos. Res.* **2018**, *207*, 28–41. [CrossRef]
21. Lu, Y.; Zhang, W.; Wang, K. Evaluation of heavy precipitation simulated by the WRF model using 4D-Var data assimilation with TRMM 3B42 and GPM IMERG over the Huaihe River Basin, China. *Remote Sens.* **2018**, *10*, 646.
22. Chen, F.; Li, X. Evaluation of IMERG and TRMM 3B43 monthly precipitation products over mainland China. *Remote Sens.* **2016**, *8*, 472. [CrossRef]
23. Prakash, S.; Gairola, R. Validation of TRMM-3B42 precipitation product over the tropical Indian Ocean using rain gauge data from the RAMA buoy array. *Theor. Appl. Climatol.* **2014**, *115*, 451–460. [CrossRef]
24. Dinku, T.; Chidzambwa, S.; Ceccato, P.; Connor, S.; Ropelewski, C. Validation of high-resolution satellite rainfall products over complex terrain. *Int. J. Remote Sens.* **2008**, *29*, 4097–4110. [CrossRef]
25. Pierre, C.; Bergametti, G.; Marticorena, B.; Mougin, E.; Lebel, T.; Ali, A. Pluriannual comparisons of satellite-based rainfall products over the Sahelian belt for seasonal vegetation modeling. *J. Geophys. Res. Atmos.* **2011**, *116*. [CrossRef]
26. Gosset, M.; Viarre, J.; Quantin, G.; Alcoba, M. Evaluation of several rainfall products used for hydrological applications over West Africa using two high-resolution gauge networks. *Q. J. R. Meteorol. Soc.* **2013**, *139*, 923–940. [CrossRef]
27. Ochoa, A.; Pineda, L.; Crespo, P.; Willems, P. Evaluation of TRMM 3B42 precipitation estimates and WRF retrospective precipitation simulation over the Pacific–Andean region of Ecuador and Peru. *Hydrol. Earth Syst. Sci.* **2014**, *18*, 3179–3193. [CrossRef]
28. Salio, P.; Hobouchian, M.P.; Skabar, Y.G.; Vila, D. Evaluation of high-resolution satellite precipitation estimates over southern South America using a dense rain gauge network. *Atmos. Res.* **2015**, *163*, 146–161. [CrossRef]
29. Blacutt, L.A.; Herdies, D.L.; de Gonçalves, L.G.G.; Vila, D.A.; Andrade, M. Precipitation comparison for the CFSR, MERRA, TRMM3B42 and Combined Scheme datasets in Bolivia. *Atmos. Res.* **2015**, *163*, 117–131. [CrossRef]
30. Satgé, F.; Bonnet, M.-P.; Gosset, M.; Molina, J.; Lima, W.H.Y.; Zolá, R.P.; Timouk, F.; Garnier, J. Assessment of satellite rainfall products over the Andean plateau. *Atmos. Res.* **2016**, *167*, 1–14. [CrossRef]
31. Kidd, C.; Bauer, P.; Turk, J.; Huffman, G.; Joyce, R.; Hsu, K.-L.; Braithwaite, D. Intercomparison of high-resolution precipitation products over northwest Europe. *J. Hydrometeorol.* **2012**, *13*, 67–83. [CrossRef]

32. Stampoulis, D.; Anagnostou, E.N.; Nikolopoulos, E.I. Assessment of high-resolution satellite-based rainfall estimates over the Mediterranean during heavy precipitation events. *J. Hydrometeorol.* **2013**, *14*, 1500–1514. [CrossRef]
33. Conti, F.L.; Hsu, K.-L.; Noto, L.V.; Sorooshian, S. Evaluation and comparison of satellite precipitation estimates with reference to a local area in the Mediterranean Sea. *Atmos. Res.* **2014**, *138*, 189–204. [CrossRef]
34. Skok, G.; Žagar, N.; Honzak, L.; Žabkar, R.; Rakovec, J.; Ceglar, A. Precipitation intercomparison of a set of satellite-and raingauge-derived datasets, ERA Interim reanalysis, and a single WRF regional climate simulation over Europe and the North Atlantic. *Theor. Appl. Climatol.* **2016**, *123*, 217–232. [CrossRef]
35. Chen, Y.; Ebert, E.E.; Walsh, K.J.; Davidson, N.E. Evaluation of TMPA 3B42 daily precipitation estimates of tropical cyclone rainfall over Australia. *J. Geophys. Res. Atmos.* **2013**, *118*, 911–966. [CrossRef]
36. Peña-Arancibia, J.L.; van Dijk, A.I.; Renzullo, L.J.; Mulligan, M. Evaluation of precipitation estimation accuracy in reanalyses, satellite products, and an ensemble method for regions in Australia and South and East Asia. *J. Hydrometeorol.* **2013**, *14*, 1323–1333. [CrossRef]
37. Pipunic, R.; Ryu, D.; Costelloe, J.; Su, C. *Evaluation of Real-Time Satellite Rainfall Products in Semi-Arid/Arid Australia*; MODSIM2013; Piantadosi, J., Anderssen, R.S., Boland, J., Eds.; Modelling and Simulation Society of Australia & New Zealand: Canberra, Australia, 2013; p. 31063112.
38. Mahmoud, M.T.; Al-Zahrani, M.A.; Sharif, H.O. Assessment of global precipitation measurement satellite products over Saudi Arabia. *J. Hydrol.* **2018**, *559*, 1–12. [CrossRef]
39. Maggioni, V.; Meyers, P.C.; Robinson, M.D. A review of merged high-resolution satellite precipitation product accuracy during the Tropical Rainfall Measuring Mission (TRMM) era. *J. Hydrometeorol.* **2016**, *17*, 1101–1117. [CrossRef]
40. Yuan, F.; Zhang, L.; Win, K.W.W.; Ren, L.; Zhao, C.; Zhu, Y.; Jiang, S.; Liu, Y. Assessment of GPM and TRMM multi-satellite precipitation products in streamflow simulations in a data-sparse mountainous watershed in Myanmar. *Remote Sens.* **2017**, *9*, 302. [CrossRef]
41. Beck, H.E.; Vergopolan, N.; Pan, M.; Levizzani, V.; van Dijk, A.I.; Weedon, G.P.; Brocca, L.; Pappenberger, F.; Huffman, G.J.; Wood, E.F. Global-scale evaluation of 22 precipitation datasets using gauge observations and hydrological modeling. *Hydrol. Earth Syst. Sci.* **2017**, *21*, 6201. [CrossRef]
42. Muhammad, W.; Yang, H.; Lei, H.; Muhammad, A.; Yang, D. Improving the regional applicability of satellite precipitation products by ensemble algorithm. *Remote Sens.* **2018**, *10*, 577. [CrossRef]
43. Hussain, Y.; Satgé, F.; Hussain, M.B.; Martinez-Carvajal, H.; Bonnet, M.-P.; Cárdenas-Soto, M.; Roig, H.L.; Akhter, G. Performance of CMORPH, TMPA, and PERSIANN rainfall datasets over plain, mountainous, and glacial regions of Pakistan. *Theor. Appl. Climatol.* **2017**, *131*, 1–14. [CrossRef]
44. Anjum, M.N.; Ding, Y.; Shangguan, D.; Ijaz, M.W.; Zhang, S. Evaluation of high-resolution satellite-based real-time and post-real-time precipitation estimates during 2010 extreme flood event in Swat River Basin, Hindukush region. *Adv. Meteorol.* **2016**, *2016*. [CrossRef]
45. Butt, M.J.; Iqbal, M.F. Impact of climate variability on snow cover: A case study of northern Pakistan. *Pak. J. Meteorol.* **2009**, *5*, 10.
46. Dimri, A.; Niyogi, D.; Barros, A.; Ridley, J.; Mohanty, U.; Yasunari, T.; Sikka, D. Western disturbances: A review. *Rev. Geophys.* **2015**, *53*, 225–246. [CrossRef]
47. Asmat, U.; Athar, H. Run-based multi-model interannual variability assessment of precipitation and temperature over Pakistan using two IPCC AR4-based AOGCMs. *Theor. Appl. Climatol.* **2017**, *127*, 1–16. [CrossRef]
48. Asmat, U.; Athar, H.; Nabeel, A.; Latif, M. An AOGCM based assessment of interseasonal variability in Pakistan. *Clim. Dyn.* **2017**, *50*, 1–25. [CrossRef]
49. Salma, S.; Shah, M.; Rehman, S. Rainfall trends in different climate zones of Pakistan. *Pak. J. Meteorol.* **2012**, *9*, 17.
50. Greene, W.H. *Econometric Analysis*; Pearson Education India: Delhi, India, 2003.
51. Gujarati, D.N. *Basic Econometrics*; Tata McGraw-Hill Education: Noida, India, 2009.
52. Huffman, G.J.; Bolvin, D.T.; Nelkin, E.J. *Day 1 IMERG Final Run Release Notes*; NASA/GSFC: Greenbelt, MD, USA, 2015.
53. Simpson, J.; Adler, R.F.; North, G.R. A proposed tropical rainfall measuring mission (TRMM) satellite. *Bull. Am. Meteorol. Soc.* **1988**, *69*, 278–295. [CrossRef]

54. Kummerow, C.; Barnes, W.; Kozu, T.; Shiue, J.; Simpson, J. The tropical rainfall measuring mission (TRMM) sensor package. *J. Atmos. Ocean. Technol.* **1998**, *15*, 809–817. [CrossRef]
55. Kummerow, C.; Simpson, J.; Thiele, O.; Barnes, W.; Chang, A.; Stocker, E.; Adler, R.; Hou, A.; Kakar, R.; Wentz, F. The status of the Tropical Rainfall Measuring Mission (TRMM) after two years in orbit. *J. Appl. Meteorol.* **2000**, *39*, 1965–1982. [CrossRef]
56. As-Syakur, A.; Tanaka, T.; Prasetia, R.; Swardika, I.; Kasa, I. Comparison of TRMM multisatellite precipitation analysis (TMPA) products and daily-monthly gauge data over Bali. *Int. J. Remote Sens.* **2011**, *32*, 8969–8982. [CrossRef]
57. Ashouri, H.; Hsu, K.-L.; Sorooshian, S.; Braithwaite, D.K.; Knapp, K.R.; Cecil, L.D.; Nelson, B.R.; Prat, O.P. PERSIANN-CDR: Daily precipitation climate data record from multisatellite observations for hydrological and climate studies. *Bull. Am. Meteorol. Soc.* **2015**, *96*, 69–83. [CrossRef]
58. Gebregiorgis, A.S.; Hossain, F. Understanding the dependence of satellite rainfall uncertainty on topography and climate for hydrologic model simulation. *IEEE Trans. Geosci. Remote Sens.* **2013**, *51*, 704–718. [CrossRef]
59. Hirpa, F.A.; Gebremichael, M.; Hopson, T. Evaluation of high-resolution satellite precipitation products over very complex terrain in Ethiopia. *J. Appl. Meteorol. Climatol.* **2010**, *49*, 1044–1051. [CrossRef]